Electrochemical characterisation of a martensitic stainless steel in a neutral chloride solution

Sabrina Marcelin, Nadine Pébère, Sophie Régnier

Electrochemical characterisation of a martensitic stainless steel in a neutral chloride solution

Sabrina Marcelin [a,1], Nadine Pébère [a,*,2], Sophie Régnier [b]

[a] Université de Toulouse, CIRIMAT, UPS/INPT/CNRS, ENSIACET, 4, Allée Emile Monso – BP 44362, 31030 Toulouse cedex 4, France
[b] Institut Catholique d'Arts et Métiers, 75, Avenue de Grande-Bretagne, 31300 Toulouse, France

A B S T R A C T

This paper focuses on the characterisation of the electrochemical behaviour of a martensitic stainless steel in 0.1 M NaCl + 0.04 M Na_2SO_4 solution and is a part of a study devoted to crevice corrosion resistance of stainless steels. Polarisation curves and electrochemical impedance measurements were obtained for different experimental conditions in bulk electrolyte. X-ray photoelectron spectroscopy (XPS) was used to analyse the passive films. At the corrosion potential, the stainless steel was in the passive state and the corrosion process was controlled by the properties of the passive film formed during air exposure. During immersion in the deaerated solution, the passive film was only slightly modified, whereas it was altered both in composition and thickness during immersion in the aerated solution. After cathodic polarisation of the stainless steel electrode surface, the oxide film was almost totally removed and the surface appeared to be uniformly active for oxygen reduction. The new passive film, formed at the corrosion potential, was enriched with iron species and less protective. Impedance diagrams allowed the characterisation of both the oxide film (high-frequency range) and the charge transfer process (low-frequency range).

Keywords:
Stainless steel
Passive film
Surface state
SIE

1. Introduction

Martensitic stainless steels are mainly used for applications where high mechanical performance is required [1,2]. However, due to their low chromium content, they are relatively sensitive to localised corrosion, particularly crevice corrosion encountered in confined environments. In these areas, oxygen is progressively consumed and cannot be renewed by diffusion or convection. Outside the confined area, the cathodic reaction of oxygen reduction still occurs on the metal surface, whereas, in the confined area, the metal surface becomes the anode. The corrosion process leads to a modification of the chemical composition of the electrolyte in the crevice with simultaneous acidification and increase of chloride ion concentration [3]. These new local conditions induce depassivation of the stainless steel and lead to severe corrosion. The crevice corrosion resistance of the stainless steels is strongly dependent on the passive film properties [4]. The substrate (nature and content of alloying elements), the environment (aerated, deaerated, neutral, acidic or alkaline) and also specific experimental conditions (*e.g.* anodic polarisation) affect both the chemical composition and the structure of the passive layer [4–8]. To obtain a better knowledge of the passive films formed on stainless steels, many studies have been devoted to chemical analysis by X-ray photoelectron spectroscopy (XPS) [9–14]. In neutral or alkaline environments, passive films are often described as duplex layers with an inner part which is enriched in chromium oxide and an outer part, in contact with the electrolyte, enriched in elemental iron (oxides and hydroxides) [12,14].

To reduce the air-formed oxide film, the stainless steels surface was often cathodically polarised, particularly to investigate passivity by Mott–Schottky analysis [15–20]. It was also reported that the reproducibility of electrochemical measurements performed on passive films was improved after cathodic polarisation [21,22]. However, the influence of this procedure on the formation of the new passive film in an electrolytic solution was not clearly indicated.

The corrosion behaviour of the stainless steels is commonly assessed by using electrochemical impedance spectroscopy (EIS) because, covering a wide frequency range, EIS yields information on different processes occurring on the metal/oxide/electrolyte interface. The impedance data obtained on stainless steels were generally analysed by using various equivalent circuits to extract quantitative parameters. However, the different elements used in the circuits were not attributed to the same phenomena. Andrade et al. [23] studied the electrochemical behaviour of steel rebars in concrete and the influence of environmental factors ($CaCl_2$ or $NaNO_2$). The impedance diagrams presented only one time constant, but the experimental data were modelled using two

* Corresponding author. Tel.: +33 5 34 32 34 23.
E-mail address: nadine.pebere@ensiacet.fr (N. Pébère).
[1] ISE student member.
[2] ISE active member.

http://dx.doi.org/10.1016/j.electacta.2012.09.011

hierarchical parallel RC circuits to obtain better agreement with the experimental data. The high-frequency time constant was associated to the corrosion process (double layer capacitance in parallel with the charge transfer resistance) and the low-frequency time constant was correlated to redox processes taking place in the passive layer. These processes involve the oxidation of the corrosion products $Fe(OH)_2$ to form magnetite (Fe_3O_4) [23]. The magnetite can also be partially oxidised to γ-FeOOH [14,23] and chemically reduced to γ-Fe_2O_3 [24]. Abreu et al. [21,24] studied the electrochemical behaviour of AISI 304L stainless steel in a deaerated 0.1 M NaOH solution. They used a hierarchical arrangement of three stacked RC pairs. The high-frequency time constant was correlated to the metal/film interface. The medium and low-frequency time constants were associated to the redox processes. Freire et al. studied the passive behaviour of AISI 316 stainless steel in alkaline aerated media [14]. According to the authors, the high-frequency time constant can be correlated with the charge transfer process or to the barrier properties of the passive film. The low-frequency time constant was associated to the redox or to the interfacial processes. For AISI 304 in alkaline solutions with different pH and in the presence of chlorides, the high-frequency time constant was assigned to the areas covered with the passive film (protective oxide); the low-frequency time constant was correlated with the active surface area (film defects or pores in the absence of chlorides and active pits in the presence of chlorides) [25]. Recently, a model which involved the presence of low-conductivity (chromium rich regions of insulating character) and high-conductivity (iron rich regions based on magnetite of conducting character) oxide areas over the metal substrate was considered to analyse the impedance data obtained on AISI 316L in sodium hypochlorite and peracetic acid solutions [26]. From recent literature, it appears that the impedance analysis on passive films still remains a subject open to discussion [25]. It can be mentioned that the main references cited above, concerned impedance results for stainless steels in alkaline media with or without chlorides. The impedance diagrams were relatively similar to those obtained in the present study in neutral chloride solutions and thus, our data can be compared with the results obtained in alkaline media.

The present work was designed to obtain a better knowledge of the electrochemical behaviour of a martensitic stainless steel in a neutral chloride electrolyte. To our knowledge, no studies have been reported in the literature concerning the corrosion behaviour of martensitic stainless steel. Polarisation curves were plotted and impedance measurements carried out using a rotating disk electrode (500 rpm). Impedance diagrams were obtained both at the corrosion potential and in the anodic and cathodic ranges. Since the martensitic stainless steels are sensitive to crevice corrosion, particular attention was paid to the influence of oxygen and experiments were performed in aerated or deaerated media. The influence of the surface state (cathodic polarisation) on the development of the passive film was also investigated. XPS analyses were carried out to determine the chemical composition of the films.

2. Experimental

2.1. Material

The composition in weight percent of the X12CrNiMoV12-3 martensitic stainless steel was C = 0.12, Cr = 11.5, Ni = 2.5, Mo = 1.6, V = 0.3 and Fe to balance.

2.2. Electrochemical measurements

The electrochemical measurements were performed using a conventional three-electrode cell. It contained a platinum grid, a saturated calomel reference electrode (SCE) and a rod of the stainless steel, of 1 cm^2 cross-sectional area, used as working electrode (rotating disk). The body of the rod was covered with a heat-shrinkable sheath leaving only the tip of the cylinder in contact with the solution. Prior to any experiment, the electrode was ground with successive SiC papers and diamond paste (grade 1000–3 μm), rinsed and sonicated with ethanol and finally dried in warm air. The electrode rotation rate was fixed at 500 rpm.

The corrosive medium was prepared from distilled water by adding 0.1 M NaCl + 0.04 M Na_2SO_4 (reagent grade). The addition of sulphate ions enabled limitation of the increase of the anodic current density when pits started to form at anodic potentials. The inhibitive effect of SO_4^{2-} anion on pitting corrosion is well known [27,28]. For deaerated experiments, the electrolytic solution was initially purged with nitrogen for 1 h and then, the working electrode was introduced into the cell. N_2 bubbling was maintained during the experiment.

Polarisation curves were plotted under potentiodynamic regulation using a Solartron 1287 electrochemical interface. The cathodic and anodic branches were plotted either consecutively, starting from the cathodic potential of −1 V/SCE, or independently from the corrosion potential (E_{corr}). In both cases, the curves were obtained at a potential sweep rate of 0.6 V/h. Electrochemical impedance measurements were carried out using a Solartron 1287 electrochemical interface connected with a Solartron 1250 frequency response analyser. Impedance diagrams were obtained over a frequency range of 65 kHz to a few mHz with eight points per decade using a 15 mV peak-to-peak sinusoidal voltage. The linearity of the system was checked by varying the amplitude of the ac signal applied to the sample. The electrochemical results were obtained from at least three experiments to ensure reproducibility. The impedance spectra were fitted by using electrical equivalent circuits with Z-view impedance software.

2.3. XPS analysis

The XPS measurements were carried out on a K-alpha Thermo Scientific spectrometer. The samples were prepared by the same procedure as for the electrochemical experiments. After 17 h of immersion, the stainless steel sample was removed from the solution, rinsed with ethanol then dried in warm air and placed in a vacuum chamber. The specimens were irradiated with the AlKα ray source ($h\nu$ = 1486.6 eV). The X-ray power was 300 W. Angle-resolved measurements were made at a take-off angle $\theta = 90^\circ$ (*e.g.* normal to the metal surface). The surface area analysed was about 1 mm^2. The experimental resolution of the binding energy was 1 eV. The Shirley method was used for background subtraction and peak deconvolution was performed using Thermo Avantage software. Binding energies were corrected for possible charging effects by referencing to the C1s (284.8 eV) peak. For each sample, three different analyses were performed to verify the homogeneity of the layer composition.

3. Results

First, polarisation curves and impedance measurements at the corrosion potential (E_{corr}) were carried out for three different experimental conditions: aerated medium, deaerated medium and in aerated medium after a cathodic polarisation for 1 h at −1 V/SCE. This last condition was applied to partly or totally reduce the oxide film naturally formed during air exposure. Then, impedance measurements were performed in the aerated solution, for different anodic and cathodic overpotentials. To characterise the initial state of the native oxide film before immersion in the aggressive solution, XPS analysis was performed on a sample just after polishing

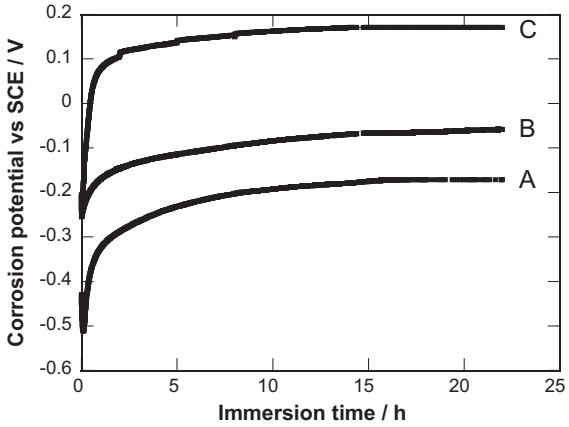

Fig. 1. Corrosion potential of X12CrNiMoV12-3 martensitic stainless steel as a function of time, (A) in deaerated 0.1 M NaCl + 0.04 M Na_2SO_4 solution, (B) in aerated solution and (C) after a cathodic polarisation (−1 V/SCE, 1 h) in aerated solution.

and cleaning. Then, XPS analyses were carried out on two different samples after 17 h of immersion in the aerated electrolyte with and without the surface treatment (polarisation at −1 V/SCE).

3.1. DC measurements

Fig. 1 illustrates the variation of the free corrosion potential, E_{corr}, of the stainless steel dipped into the aggressive solution for the three experimental conditions. In all cases, the shape of the curves is similar. During the first 5 h of immersion, E_{corr} increases significantly with time and then progressively stabilises after 15–20 h of immersion. The time required to reach the stationary state is relatively long (one day) which is in agreement with different works reported in the literature for different types of stainless steel [14,29,30]. The values of E_{corr}, after 23 h of immersion, are −0.16 V/SCE for the sample in deaerated solution (curve A), −0.06 V/SCE for the sample in aerated medium (curve B) and 0.17 V/SCE for the sample after cathodic polarisation in aerated medium (curve C). The shift of E_{corr} in the cathodic direction, observed in deaerated medium, is attributed to the decrease of the cathodic current density. In aerated medium, E_{corr} strongly depends on the surface state. After 23 h of immersion, it was shifted by about 230 mV in the anodic direction when the electrode was polarised at −1 V/SCE (curve C) by comparison with the sample which was not previously polarised (sample B).

Fig. 2 shows the polarisation curves for the martensitic stainless steel obtained after 2 h of immersion in aerated medium and plotted either from E_{corr} or from −1 V/SCE to E_{pit}. The curves differ according to the potential scan. In the cathodic domain, when the curve is plotted from E_{corr}, a pseudo plateau due to oxygen reduction is observed around −0.7 to −0.8 V/SCE. Then, at about −0.8 V/SCE, an increase of the cathodic current density is observed. This behaviour is explained by the contribution of the cathodic reduction of the oxide film formed during immersion [31,32]. This is confirmed by the fact that when the curve is plotted from the cathodic potential, the current density is significantly higher and its value at −1 V/SCE (100 μA cm^{-2}) corresponds to that obtained on a uniformly active surface according to the Levich theory [33]. Thus, it can be concluded that in the present study, during the cathodic plot from −1 V/SCE to E_{corr} or when the electrode is polarised at −1 V/SCE, most of the oxides are reduced and the surface becomes totally active for oxygen reduction.

In the anodic domain, for both curves, a passivity plateau is observed before an abrupt increase of the current density due to the breakdown of the passive film and to the development of pits. The anodic current density for the curve plotted from −1 V/SCE

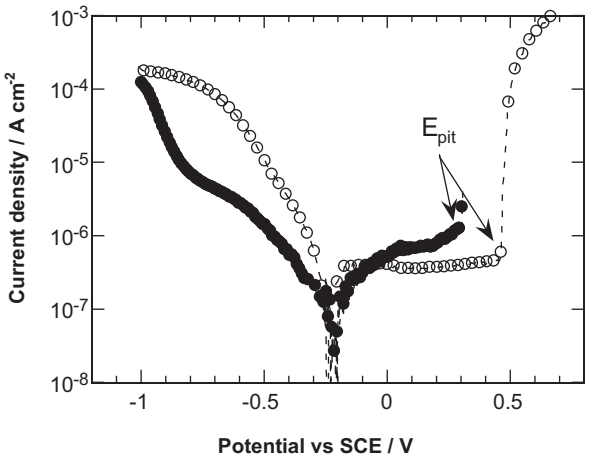

Fig. 2. Polarisation curves obtained for the martensitic stainless steel after 2 h of immersion in the aerated solution: (●) from E_{corr} (the cathodic and anodic branches were obtained separately) and (○) from −1 V/SCE to E_{pit} (the cathodic and anodic branches were obtained consecutively).

(0.4 μA cm^{-2}) is of the same order of magnitude as that measured for the curve plotted from E_{corr} (0.7 μA cm^{-2}). In addition, the difference in the pitting potential (E_{pit}) is not significantly modified for the two experimental procedures. Generally, the pitting potential is not a reproducible parameter [34].

Fig. 3 compares the polarisation curves for the martensitic stainless steel obtained after 17 h of immersion at E_{corr} in aerated and deaerated electrolytes. The cathodic current density is lower and E_{corr} is shifted towards cathodic values when the medium is deaerated. The anodic current density on the plateau is approximately the same in both media (0.5–0.6 μA cm^{-2}). In deaerated electrolyte, the passivity plateau is larger due to the shift of E_{corr} in the cathodic direction. In these two curves, the difference observed in E_{pit} cannot be discussed as mentioned earlier. However, it can be seen, by comparison with the anodic curve plotted after 2 h of immersion (Fig. 2), that E_{pit} is shifted towards more anodic values after 17 h of immersion indicating a modification of the passive film with increasing immersion time. From Fig. 3, it can be concluded that the anodic branches are relatively similar in aerated and deaerated media. The anodic branch plotted after a preliminary polarisation at −1 V/SCE and 17 h of immersion at E_{corr} is also reported in Fig. 3 and reveals both an increase of the anodic current density to reach

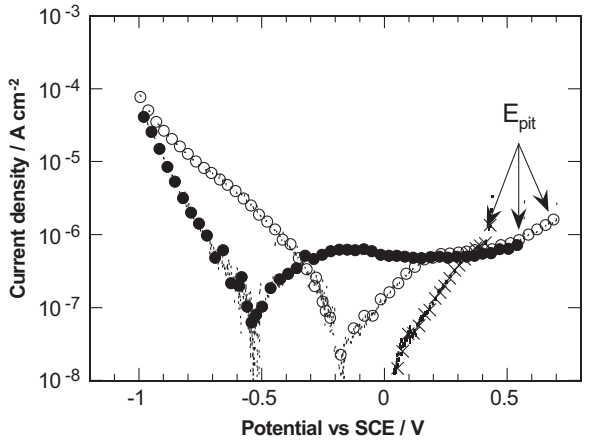

Fig. 3. Polarisation curves obtained for the martensitic stainless steel after 17 h of immersion: (○) aerated medium, (●) deaerated medium and (×) after a cathodic polarisation at −1 V/SCE in aerated medium (in all cases the cathodic and the anodic branches were obtained separately).

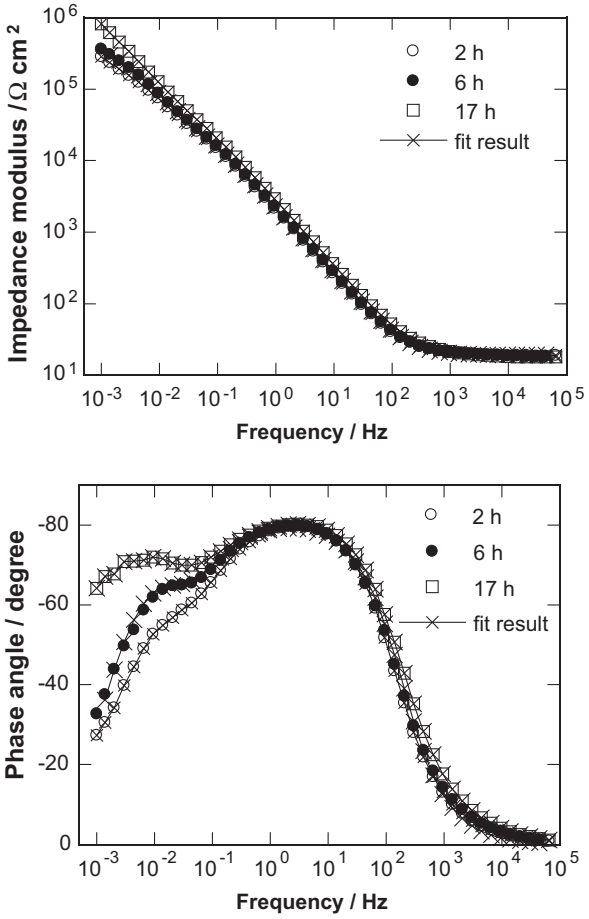

Fig. 4. Electrochemical impedance diagrams obtained at E_{corr} after different hold times in the aerated solution.

about 2 μA cm^{-2} and a short passivity plateau by comparison with the two other curves.

3.2. Electrochemical impedance measurements

In this section, impedance measurements were first performed at E_{corr} under the same experimental conditions as the polarisation curves (aerated and deaerated media, and with a pre-polarisation of the electrode at −1 V/SCE). Fig. 4 shows the impedance diagrams plotted *versus* immersion time in the aerated solution after surface polishing only. Independently of the immersion time, the diagrams are characterised by two time constants. The two time constants are better defined and the impedance modulus in the low-frequency range increases with the immersion time. For longer immersion times (>17 h), the impedance diagrams are relatively similar and are not reported here. The impedance diagrams were also obtained for the martensitic stainless steel after polarisation at −1 V/SCE and for different immersion times at E_{corr} in the aerated solution. In this case, the diagrams are poorly dependent on the immersion time and only the diagram obtained after 17 h of immersion is shown in Fig. 5. By comparison with the diagrams reported in Fig. 4, it can be seen that the two time constants are better separated and the modulus at low frequency is of the same order of magnitude (about 10^6 Ω cm^2). The impedance diagram obtained in the deaerated solution for the stainless steel after 17 h of immersion at corrosion potential (Fig. 6) shows that the time constant at low frequency disappears and it can be noted that the impedance modulus at low frequency is approximately the same as in aerated medium. Thus, it can be concluded

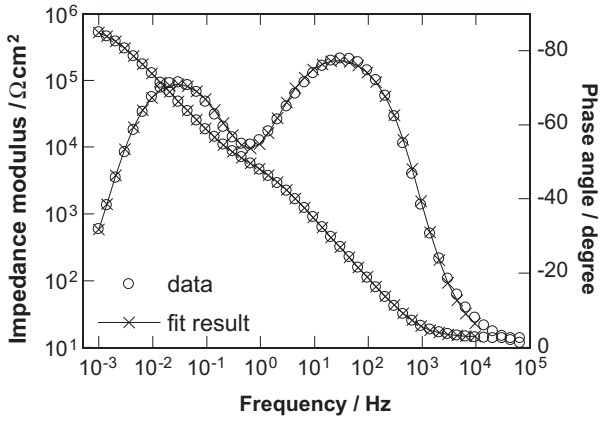

Fig. 5. Electrochemical impedance diagram obtained after a preliminary cathodic polarisation at −1 V/SCE for 1 h of the stainless steel and then 17 h of immersion at E_{corr} (aerated solution).

that the low-frequency time constant is linked to the presence of oxygen in the electrolytic solution.

El-Egamy and Badaway [27] have proposed an equivalent circuit composed of an R//CPE element to describe the behaviour of 304 stainless steel in a sodium sulphate solution. The time constant was associated to the response of the passive film. This simple model was used to fit the impedance data obtained in a deaerated medium (Fig. 7a). Then, to take into account the presence of the second time constant in the low-frequency range, an additional R//CPE circuit was introduced (Fig. 7b). The two parts of the circuit were imbricated to take into account the oxygen contribution and the progressive modification of the passive film as described in the literature [35–37]. Thus, the time constant in the high-frequency range was attributed to the oxide film (R_{ox}, α_{ox} and Q_{ox}) and the time constant in the low-frequency range was attributed to the charge transfer reaction: oxidation of the substrate/oxygen reduction (R_t, α_{dl} and Q_{dl}).

Some parameters (α_{ox}, Q_{ox}, α_{dl} and Q_{dl}) were graphically extracted [38]. The same values were obtained from the equivalent circuits by the fitting procedure. The experimental diagrams are well fitted with the equivalent circuits, as can be seen in Figs. 4, 5 and 6. Thus, the values of the parameters can be extracted and discussed. They are reported in Tables 1, 2 and 3 corresponding to Figs. 4, 5 and 6, respectively. For the different experimental conditions, the α_{ox} values are relatively similar (about 0.9) and do not depend on the immersion time. The Q_{ox} values decrease with immersion time for the three experimental conditions. This

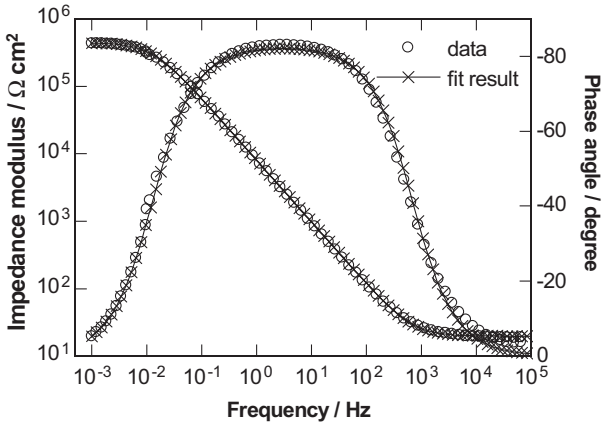

Fig. 6. Electrochemical impedance diagram obtained at E_{corr} after 17 h of immersion (deaerated solution).

Table 1
Fitted parameters values obtained at E_{corr} for the martensitic stainless steel as a function of the exposure time to the aerated solution.

Immersion time (h)	α_{ox} ±0.3%	Q_{ox} ($M\Omega^{-1}$ cm^{-2})s^{α} ±1%	R_{ox} ($k\Omega$ cm^2) ±11%	α_{dl} ±4%	Q_{dl} ($M\Omega^{-1}$ cm^{-2})s^{α} ±12%	R_t ($k\Omega$ cm^2) ±5%
2	0.90	90	50	0.82	90	260
6	0.90	87	62	0.84	64	400
10	0.90	86	76	0.88	61	510
17	0.90	76	110	0.89	42	1680

Table 2
Fitted parameters values obtained at E_{corr} for the martensitic stainless steel as a function of the exposure time to the aerated solution (a cathodic polarisation at −1 V/SCE for 1 h was previously applied to the stainless steel).

Immersion time (h)	α_{ox} ±0.2%	Q_{ox} ($M\Omega^{-1}$ cm^{-2})s^{α} ±1%	R_{ox} ($k\Omega$ cm^2) ±5%	α_{dl} ±1.3%	Q_{dl} ($M\Omega^{-1}$ cm^{-2})s^{α} ±1.3%	R_t ($k\Omega$ cm^2) ±3%
2	0.91	32	6.1	0.73	63	110
6	0.91	29	7.2	0.81	64	260
10	0.91	27	7.3	0.83	64	470
17	0.91	26	7.7	0.87	64	700

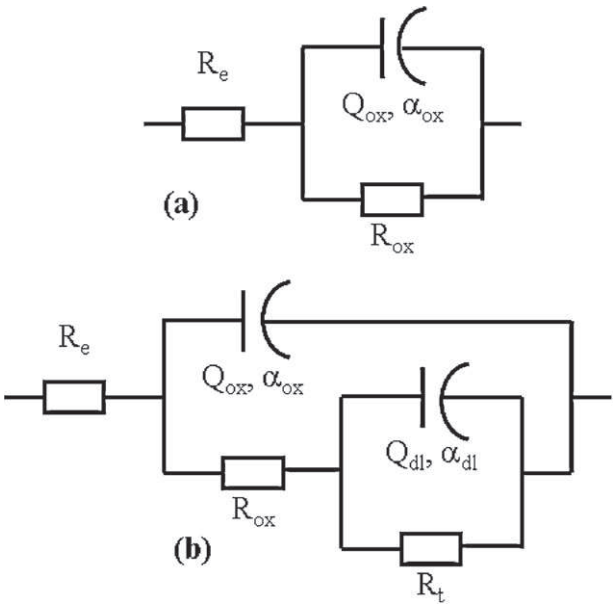

Fig. 7. Equivalent circuits used to fit the experimental impedance data obtained in (a) deaerated and (b) aerated media.

indicates a modification of the passive layer (thickening and/or modification of the composition of the film). The values of Q_{ox} are relatively high for oxide capacity. However, the CPE parameter, Q, cannot be attributed to a capacity. Similar values of Q_{ox} were already reported for a Fe17Cr stainless steel [39]. To explain the CPE behaviour, the authors proposed a normal distribution of local resistivity through the passive film with strong differences in resistivity between the metal/film interface and the film/electrolyte interface, due to the semiconductor character of the passive layer. This analysis partly corroborates the recent work of Guitiàn et al. [26]. The decrease of Q_{ox} is accompanied by an increase of R_{ox} with increasing immersion time. In deaerated medium, the variations of R_{ox} and Q_{ox} with immersion time are limited by comparison with those observed in aerated medium. R_{ox} values obtained after the cathodic pre-treatment are small compared to those obtained for the two other conditions and they did not significantly change with immersion whereas the values of Q_{ox} are comparable to those obtained in the deaerated medium. This indicates that the passive film formed in the electrolyte (after cathodic polarisation) is different from the film formed in the air and then exposed to the electrolytic solution. The values of R_t are also dependent on the experimental conditions. From 2 h to 17 h, R_t increased from 260 to 1700 $k\Omega$ cm^2 when the electrode was not submitted to cathodic polarisation and from 110 to 700 $k\Omega$ cm^2 when the oxide film was developed in the solution after cathodic polarisation.

Then, impedance measurements were performed in the anodic and cathodic domains to validate the impedance analysis at the corrosion potential. These measurements were only obtained in aerated medium without a preliminary polarisation at −1 V/SCE. Fig. 8 shows impedance diagrams obtained on the stainless steel for two anodic potentials: −0.2 V/SCE (close to E_{corr}) and +0.4 V/SCE (on the passivity plateau). The time constant in the high-frequency range was shifted towards higher frequencies and the time constant in the low-frequency range disappeared when the potential increased. The values obtained for the parameters associated to the high-frequency loop are reported in Table 4. It can be seen that R_{ox} increased and Q_{ox} decreased when the potential became increasingly anodic. These results can be explained by a thickening of the oxide film by the anodic polarisation and confirm the attribution of the high-frequency time constant to the passive film response. Two impedance diagrams obtained in the cathodic range (Fig. 9) show that the two time constants are modified and the impedance

Table 3
Fitted parameters values obtained at E_{corr} for the martensitic stainless steel as a function of the exposure time to the deaerated solution.

Immersion time (h)	α_{ox} ±0.1%	Q_{ox} ($M\Omega^{-1}$ cm^{-2})s^{α} ±0.6%	R_{ox} ($k\Omega$ cm^2) ±1.7%
6	0.90	30	330
10	0.91	26	388
17	0.92	23	443

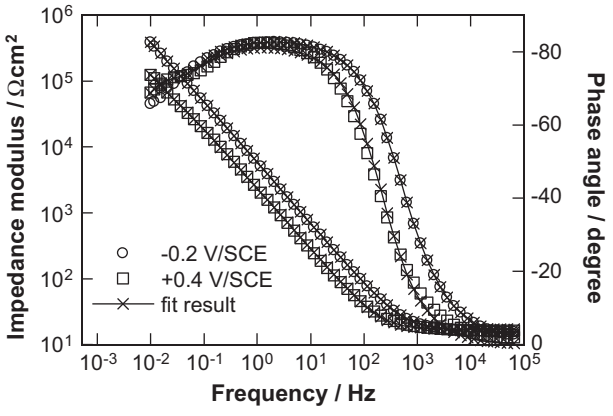

Fig. 8. Electrochemical impedance diagrams obtained in the anodic domain, after 17 h of immersion at E_{corr} (aerated solution).

Table 4
Fitted parameters values obtained for the martensitic stainless steel after 17 h of immersion and for different anodic potentials (aerated solution).

Applied potential (V/SCE)	α_{ox} ±0.3%	Q_{ox} ($M\Omega^{-1}$ cm^{-2})s^{α} ±1%	R_{ox} ($k\Omega$ cm^2) ±1.5%
−0.2	0.89	84	270
0	0.90	70	400
+0.1	0.91	50	420
+0.2	0.92	39	483
+0.4	0.92	33	782

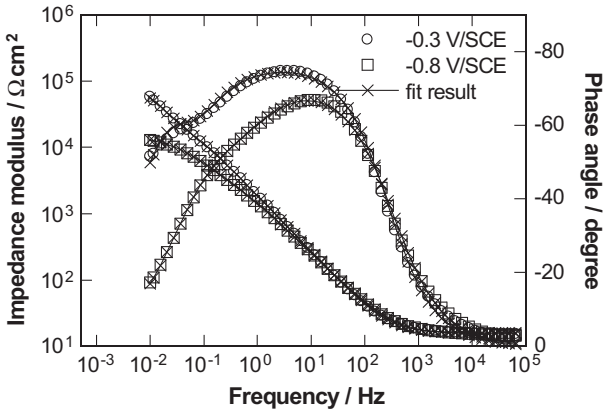

Fig. 9. Electrochemical impedance diagrams obtained in the cathodic domain, after 17 h of immersion at E_{corr} (aerated solution).

modulus strongly decreases when the potential becomes more cathodic. The values obtained for the parameters associated to the high-frequency loop are reported in Table 5 for different cathodic potentials. It can be seen that the values of Q_{ox} increase and R_{ox} decrease when the potential decreases. The significant modification of the two parameters can be explained by the progressive reduction of the oxide film in agreement with the polarisation curves (Fig. 2).

3.3. XPS analyses

Fig. 10 shows the X-ray photoelectron spectra of O1s, $Fe2p_{3/2}$ and $Cr2p_{3/2}$ for the martensitic stainless steel passive film formed in contact with air. Similar spectra were obtained for the stainless steel surface after immersion in the aerated solution with or without previous cathodic polarisation of the electrode.

The parameters used for the deconvolution of the experimental XPS spectra and the atomic percent of the species constituting the passive films are reported in Table 6. The films are mainly composed of oxides (FeO, Fe_2O_3 and Cr_2O_3), hydroxides (FeOOH and $Cr(OH)_3$) and contaminants (C═O) (Fig. 10). It is known that the Fe^{3+} contribution from Fe_2O_3 and Fe_3O_4 is difficult to identify on XPS spectra [14,22] and a global value for the two iron oxides was considered. It can be noted that after immersion in the electrolyte, ions from the solution (sodium and sulphur only) were

Table 5
Fitted parameters values obtained for the martensitic stainless steel after 17 h of immersion and for different cathodic potentials (aerated solution).

Applied potential (V/SCE)	α_{ox} ±0.2%	Q_{ox}($M\Omega^{-1}$ cm^{-2})s^{α} ±1%	R_{ox} ($k\Omega$ cm^2) ±5%
−0.3	0.85	110	38
−0.4	0.85	122	34
−0.5	0.84	127	27
−0.6	0.80	140	5
−0.8	0.81	140	3

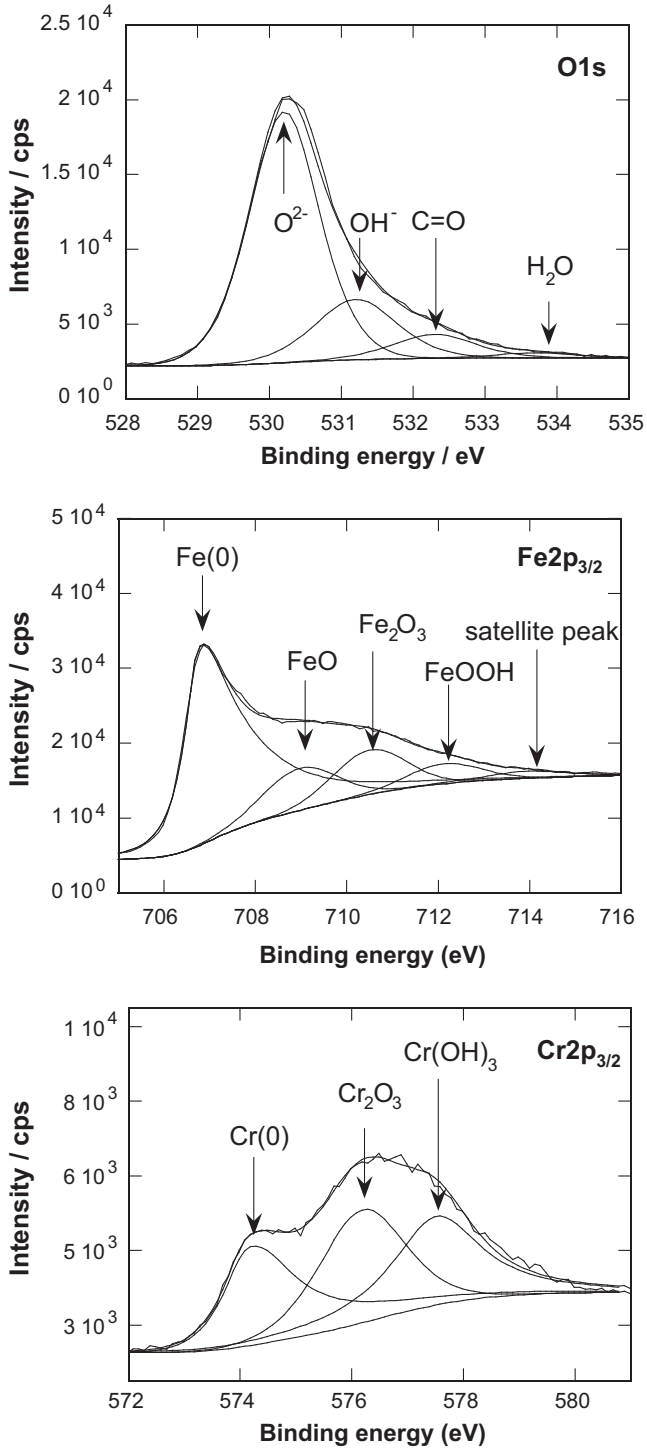

Fig. 10. Experimental and fitted O1s, $Fe2p_{3/2}$ and $Cr2p_{3/2}$ XPS spectra of martensitic stainless steel only in contact with air.

detected. The presence of molybdenum and nickel is also observed for the two immersed samples with similar atomic percent content. Fe/Cr ratios were calculated from XPS data (Table 6). For the film formed in contact with air, the Fe/Cr ratio is the highest (7.2). After immersion in the aerated solution, the ratio decreases to 1.5. Thus, the film is impoverished in iron oxides and hydroxide and enriched in chromium oxide and hydroxide after immersion in the electrolyte. This modification can be explained by the partial dissolution of the iron species present in the film during immersion [10,17,40]. The film formed in the electrolyte after the cathodic

Table 6
Parameters used for deconvolution of XPS spectra for the main species present in the passive films, atomic percent (%) of the films composition and Fe/Cr ratio obtained for the three systems.

Components	Film formed in contact with air			Film formed in aerated solution at E_{corr}			Film formed after cathodic polarisation then immersed in aerated solution at E_{corr}		
	Binding energy (eV)	FWHM[a] (eV)	(%)	Binding energy (eV)	FWHM[a] (eV)	(%)	Binding energy (eV)	FWHM[a] (eV)	(%)
Fe^0	706.5	1.2	4.0	706.6	1.2	3.4	706.5	1.2	2.2
FeO	709.5	2.0	13.6	709.6	2.0	5.4	709.6	2.0	8.5
Fe_2O_3	711.1	2.0	11.4	711.1	2.0	5.0	711.0	2.0	8.1
FeOOH	712.5	2.0	2.5	712.5	2.0	0.9	712.6	2.0	1.9
Satellite peak	714.8	2.9	2.4	714.7	2.9	0.7	714.7	2.8	1.4
Cr^0	574.1	1.4	0.9	573.9	1.2	0.7	573.8	0.4	0.4
Cr_2O_3	576.1	1.8	2.4	576.1	4.5	4.5	576.1	1.9	2.3
$Cr(OH)_3$	577.5	1.8	1.4	577.5	1.8	3.2	577.5	1.9	1.6
$Mo3d_{5/2}$	232.7	4.5	0.7	232.7	4.5	1.1	232.7	4.5	1.0
$Ni2p_{3/2}$	–	–	–	852.7	1.2	0.6	852.6	0.9	0.2
O^{2-}	530.2	1.3	45.2	530.2	1.3	32.9	530.2	1.3	37.1
OH^-	531.2	1.4	6.3	531.4	1.4	6.9	531.2	1.4	5.9
$S2p_{3/2}$	–	–	–	169.2	1.9	4.4	169.8	1.9	2.4
Na1s	–	–	–	1072.0	1.8	11.6	1072.6	1.9	6.2
Contaminants			9.2			18.7			20.8
Total (%)			100			100			100
Fe/Cr ratio	7.2			1.5			4.7		

G/L: ratio of Gaussian and Lorentzian function (G/L = 0.3 for deconvolution of $Cr2p_{3/2}$ XPS spectrum, 0.5 for deconvolution of $Fe2p_{3/2}$ and O1s XPS spectrum).
[a] FWHM: full width at half maximum.

polarisation is enriched in iron oxides and hydroxide and impoverished in chromium oxide and hydroxide (Fe/Cr ratio = 4.7) by comparison with the sample immersed in the aerated solution (Fe/Cr ratio = 1.5). As previously mentioned, the cathodic polarisation led to a surface totally active for the cathodic reaction thus facilitating iron oxidation (Fe^{2+} species) when the electrode was held at the corrosion potential for 17 h, explaining the significant quantity of iron oxides and hydroxide in the passive film for this experimental procedure.

A procedure to estimate the film thicknesses was used, similar to that reported by several authors [13,17,40]. An average thickness of 3 nm was obtained for the three experimental conditions. It must be underline that, before the introduction of the samples in the XPS chamber, the passive films formed in the electrolyte can be modified during air exposure, and the estimated thickness for the film formed during air exposure cannot be directly compared with the thickness of the films developed in the electrolyte at the corrosion potential. This is confirmed by the XPS data (Table 6) which revealed that the films formed in the solution are composed of additional species coming from the electrolyte or of contamination. As a consequence, the XPS results must be considered carefully to be compared with the electrochemical results.

4. Discussion

The impedance diagrams obtained on the martensitic stainless steel in aerated electrolyte were characterised by two time constants which were more or less distinct depending on the

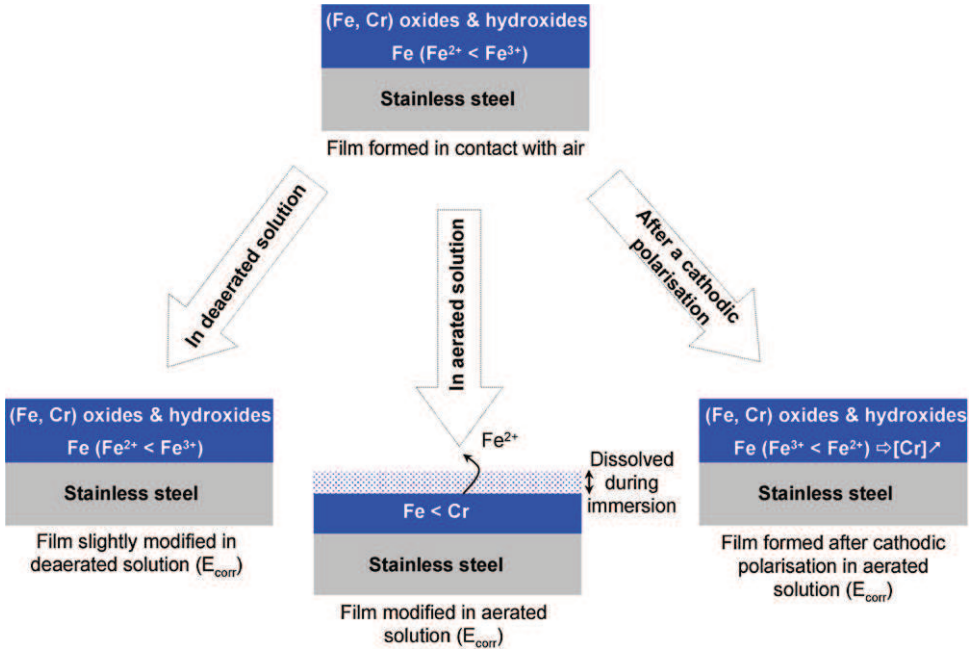

Fig. 11. Schematic illustration of the passive films formed under different conditions based on impedance results and XPS analyses (films composition).

experimental procedure. The high-frequency time constant was attributed to the properties of the oxide film. The magnitude of the R_{ox} values could be linked to the film composition, whereas Q_{ox} could be indicative of the film thickness. The low-frequency time constant was attributed, in aerated conditions, to the charge transfer process [26,31]. In deaerated medium, the charge transfer process was limited, due to the lack of oxygen, and the impedance diagrams characterised the passive film only. These different points validate the two proposed equivalent circuits to analyse the impedance data (Fig. 7). In deaerated medium, R_{ox} and Q_{ox} slowly evolved with immersion time (Table 3) and the values of R_{ox} were high (300–400 $k\Omega\,cm^2$) compared to those measured for the other conditions. This suggests that the film formed in air was only slightly modified in the electrolyte due to the absence of oxygen. In deaerated condition, the oxide film is thought to remain close to that formed in air (composition and thickness). In contrast, in aerated conditions, the passive film formed in air was progressively modified during the immersion. The values of R_{ox} were lower and Q_{ox} higher (Table 1) than in deaerated medium (Table 3). Thus, the passive film developed in aerated solution is assumed to be thinner than the film formed in deaerated medium. The film grown in solution after the cathodic polarisation appeared strongly different as underlined by the value of R_{ox} (Table 2). XPS results revealed a high iron oxides and hydroxide content due to higher corrosion of the stainless steel. This film is less protective as underlined by the high passivity current and the pitting potential which was less anodic than for the two other conditions (Fig. 3). The significant shift of E_{corr} in the anodic direction (Fig. 1, curve C) can thus be explained by the cathodic currents which are higher because the surface is more active after the removal of the oxides (Fig. 2).

In aerated condition, without the pre-polarisation of the surface, the values of R_t were high and increased significantly with immersion time (Table 1). The passive layer, enriched in chromium oxide and hydroxide (Fe/Cr ratio = 1.5), impedes the charge transfer process and thus explain the increase of R_t with immersion time. In contrast, the lower values of R_t for the sample with preliminary cathodic polarisation (Table 2) corroborates the higher corrosion rate and the fact that the layer was enriched in iron oxides and hydroxide and impoverished in chromium oxide and hydroxide (Fe/Cr ratio = 4.7). Fig. 11 presents a schematic illustration of the passive films formed under the different conditions to summarise the different points discussed above.

In conclusion, from the data reported in Tables 1, 2 and 3 it can be emphasised that in deaerated medium, the passive film confers high protection to the stainless steel and the film was only slightly modified with immersion time. When the film formed in air was exposed to the aggressive solution, an improvement of its protective effect was observed with increasing immersion time and the corrosion resistance was also high. Finally, after cathodic polarisation, the film grown in the aggressive medium was less protective as shown by the low R_{ox} and R_t values, and also by the high passivity current (Fig. 3). It must also be underlined that, independently of the experimental procedure, the passive character of the films was shown by the high values of R_{ox} (Tables 1 and 3) in spite of the low Cr content.

5. Conclusions

In this work, the behaviour of a martensitic stainless steel was studied by electrochemical techniques and XPS analyses in a neutral sodium chloride solution. Dissolved oxygen plays an important role on the formation and/or modification of the passive film during immersion in the electrolytic solution, at the corrosion potential. The two time constants, observed in the impedance diagrams in the high and low-frequency ranges, are attributed to the oxide film and to the charge transfer, respectively. The results obtained in the anodic and cathodic ranges combined with the XPS analyses corroborate the impedance results at the corrosion potential. The equivalent circuits used to analyse the impedance data provided quantitative information on the stainless steel/passive films/electrolyte interfaces. However, the CPE behaviour observed in the impedance response of the passive films should be better interpreted to give a physical meaning for the passive film response. Following studies will focus on crevice corrosion using a thin-layer cell [41].

Acknowledgments

This work was carried out in the framework of the ARCAM project, with the financial support of DGCIS, Regions Aquitaine, Auvergne and Midi-Pyrénées. The authors gratefully acknowledge the partners of the project: Ratier-Figeac, Aubert & Duval, Olympus, the Mechanical and Engineering Institute of Bordeaux, the Materials Department of ICAM and the Institute Carnot CIRIMAT. The authors thank Jérôme Esvan (CIRIMAT) for XPS analyses.

References

[1] D. Thibault, P. Bocher, M. Thomas, Residual stress and microstructure in welds of 13%Cr-4%Ni martensitic stainless steel, Journal of Materials Processing Technology 209 (2009) 2195.
[2] X.P. Ma, L.J. Wang, C.M. Liu, S.V. Subramanian, Microstructure and properties of $13Cr_5Ni1Mo0.025Nb0.09V0.06N$ super martensitic stainless steel, Materials Science and Engineering A 539 (2012) 271.
[3] J.R. Oldfield, W.H. Sutton, Crevice corrosion of stainless steels-J. A. Mathematical mode, British Corrosion Journal 13 (1978) 13.
[4] P. Schmuki, S. Virtanen, H.S. Isaacs, M.P. Ryan, A.J. Davenport, H. Böhni, T. Stenberg, Electrochemical behaviour of Cr_2O_3/Fe_2O_3 artificial passive films studied by in situ XANES, Journal of the Electrochemical Society 145 (1998) 791.
[5] V. Maurice, W.P. Yang, P. Marcus, X-ray photoelectron spectroscopy and scanning tunnelling microscopy study of passive films formed on (100)Fe-l8Cr-l3Ni single-crystal surfaces, Journal of the Electrochemical Society 145 (1998) 909.
[6] T. Ohtsuka, H. Yamada, Effect of ferrous ion in solution on the formation of anodic oxide film on iron, Corrosion Science 40 (1998) 1131.
[7] J.S. Kim, E.A. Cho, H.S. Kwan, Photoelectrochemical study on the passive film on Fe, Corrosion Science 43 (2001) 1403.
[8] N. Le Bozec, C. Compère, M. L'Her, A. Laouenan, D. Costa, P. Marcus, Influence of stainless steel surface treatment on the oxygen reduction reaction in seawater, Corrosion Science 43 (2001) 765.
[9] A. Nishikata, Y. Ichihara, T. Tsuru, Electrochemical impedance spectroscopy of metals covered with a thin electrolyte layer, Electrochimica Acta 41 (1996) 1057.
[10] K. Asami, K. Hashimoto, An X-ray photo-electron spectroscopic study of surface treatments of stainless steels, Corrosion Science 19 (1979) 1007.
[11] M. Stratmann, H. Streckel, On the atmospheric corrosion of metals which are covered with thin electrolyte layers - I. Verification of the experimental technique, Corrosion Science 30 (1990) 681.
[12] G. Lorang, M. Da Cuhna Belo, A.M.P. Simoés, Chemical composition of passive films on AISI 304 stainless steel, Journal of the Electrochemical Society 141 (1994) 3347.
[13] A. Ithurbide, I. Frateur, A. Galtayries, P. Marcus, XPS and flow-cell EQCM study of albumin adsorption on passivated chromium surfaces: influence of potential and pH, Electrochimica Acta 53 (2007) 1336.
[14] L. Freire, M.J. Carmezim, M.G.S. Ferreira, M.F. Montemor, The passive behaviour of AISI 316 in alkaline media and the effect of pH: a combined electrochemical and analytical study, Electrochimica Acta 55 (2010) 6174.
[15] S.F. Yang, D.D. Macdonald, Theoretical and experimental studies of the pitting of type 316L stainless steel in borate buffer solution containing nitrate ion, Electrochimica Acta 52 (2007) 1871.
[16] A. Fattah-Alhosseini, M.A. Golozar, A. Saatchi, K. Raeissi, Effect of solution concentration on semiconducting properties of passive films formed on austenitic stainless steels, Corrosion Science 52 (2010) 205.
[17] R.-H. Jung, H. Tsuchiya, S. Fujimoto, XPS characterization of passive films formed on Type 304 stainless steel in humid atmosphere, Corrosion Science 58 (2012) 62.
[18] Z. Feng, X. Cheng, C. Dong, L. Xu, X. Li, Passivity of 316L stainless steel in borate buffer solution studied by Mott–Schottky analysis, atomic absorption spectrometry and X-ray photoelectron spectroscopy, Corrosion Science 52 (2010) 3646.
[19] V. Vignal, O. Delrue, O. Heintz, J. Peultier, Influence of the passive film properties and residual stresses on the micro-electrochemical behavior of duplex stainless steels, Electrochimica Acta 55 (2010) 7118.

[20] H. Luo, C.F. Dong, K. Xiao, X.G. Li, Characterization of passive film on 2205 duplex stainless steel in sodium thiosulphate solution, Applied Surface Science 258 (2011) 631.
[21] C.M. Abreu, M.J. Cristóbal, R. Losada, X.R. Nóvoa, G. Pena, M.C. Pérez, Comparative study of passive films of different stainless steels developed on alkaline medium, Electrochimica Acta 49 (2004) 3049.
[22] L. Freire, X.R. Nóvoa, M.F. Montemor, M.J. Carmezim, Study of passive films formed on mild steel in alkaline media by the application of anodic potentials, Materials Chemistry and Physics 114 (2009) 962.
[23] C. Andrade, M. Keddam, X.R. Nóvoa, M.C. Pérez, C.M. Rangel, H. Takenouti, Electrochemical behaviour of steel rebars in concrete: influence of environmental factors and cement chemistry, Electrochimica Acta 46 (2001) 3905.
[24] C.M. Abreu, M.J. Cristóbal, R. Losada, X.R. Nóvoa, G. Pena, M.C. Pérez, The effect of Ni in the electrochemical properties of oxide layers grown on stainless steels, Electrochimica Acta 51 (2006) 2991.
[25] L. Freire, M.J. Carmezim, M.G.S. Ferreira, M.F. Montemor, The electrochemical behaviour of stainless steel AISI 304 in alkaline solutions with different pH in the presence of chlorides, Electrochimica Acta 56 (2011) 5280.
[26] B. Guitiàn, X.R. Nóvoa, B. Puga, Electrochemical Impedance spectroscopy as a tool for materials selection: water for haemodialysis, Electrochimica Acta 56 (2011) 7772.
[27] S.S. El-Egamy, W.A. Badaway, Passivity and passivity breakdown of 304 stainless steel in alkaline sodium sulphate solutions, Journal of Applied Electrochemistry 24 (2004) 1153.
[28] J.-L. Trompette, L. Arurault, S. Fontorbes, L. Massot, Influence of the anion specificity on the electrochemical corrosion of anodized aluminum substrates, Electrochimica Acta 55 (2010) 2901.
[29] G. Blanco, A. Bautista, H. Takenouti, EIS study of passivation of austenitic and duplex stainless steels reinforcements in simulated pore solutions, Cement & Concrete Composites 28 (2006) 212.
[30] M. Sànchez-Moreno, H. Takenouti, J.J. García-Jareño, F. Vicente, C. Alonso, A theoretical approach of impedance spectroscopy during the passivation of steel in alkaline media, Electrochimica Acta 54 (2009) 7222.
[31] C.M. Abreu, M.J. Cristóbal, R. Losada, X.R. Nóvoa, G. Pena, M.C. Pérez, High frequency impedance spectroscopy study of passive films formed on AISI 316 stainless steel in alkaline medium, Journal of Electroanalytical Chemistry 572 (2004) 335.
[32] Y.P. Kim, M. Fregonèse, H. Mazille, D. Feron, G. Santarini, Study of oxygen reduction on stainless steel surfaces and its contribution to acoustic emission recorded during corrosion processes, Corrosion Science 48 (2006) 3945.
[33] V.G. Levich, The theory of concentration polarization, Acta Physicochimica URSS 17 (1942) 257.
[34] S. Frangini, N. De Cristofaro, Analysis of the galvanostatic polarization method for determining reliable pitting potentials on stainless steels in crevice-free conditions, Corrosion Science 45 (2003) 2769.
[35] G. Okamoto, Passive film of 18-8 stainless steel structure and its function, Corrosion Science 13 (1973) 471.
[36] M. Sakashita, N. Sato, The effect of molybdate anion on the ion-selectivity of hydrous ferric oxide films in chloride solutions, Corrosion Science 17 (1977) 473.
[37] H.H. Uhlig, Passivity in metals and alloys, Corrosion Science 19 (1979) 777.
[38] M.E. Orazem, N. Pébère, B. Tribollet, A new look at graphical representation of impedance data, Journal of the Electrochemical Society 153 (2006) B129.
[39] B. Hirschorn, M.E. Orazem, B. Tribollet, V. Vivier, I. Frateur, M. Musiani, Constant-phase-element behavior caused by resistivity distributions in films: 2. Applications, Journal of the Electrochemical Society 157 (2010) C458.
[40] R. Kirchheim, B. Heine, H. Fischmeister, S. Hofmann, H. Knote, U. Stolz, The passivity of iron-chromium alloys, Corrosion Science 29 (1989) 899.
[41] E. Remita, E. Sutter, B. Tribollet, F. Ropital, X. Longaygue, C. Taravel-Condat, N. Desamais, A thin layer cell adapted for corrosion studies in confined aqueous environments, Electrochimica Acta 52 (2007) 7715.